

DEVELOPMENT OF THE PREDICTION MODEL FOR ACID RAIN AND SNOW CONSIDERING THE DETAILED CLOUD MICROPHYSICAL PROCESSES

By

S. Oishi

University of Yamanashi , Kofu, Yamanashi, Japan

M. Matsui

Osaka Municipal Government, Osaka, Japan

and

S. Ikebuchi

Kyoto University, Kyoto, Japan

SYNOPSIS

Recently acid rain and snow have become major global and environmental issues. Many prediction models for acid rain have been proposed. Most of them use the bulk water type method, which is known as the bulk method, for microphysical processes. However, the size distribution of cloud droplets is an important factor when considering the transportation and transformation of acidic species among different phases of water, that is., water vapor, liquid drop and ice (snow). The size distribution of cloud droplets is calculated by the explicit type microphysical process method, which is also known as the bin method. Therefore, in this study we developed a prediction model for acid rain and snow by means of the bin method. Moreover, we also investigated the mechanism of acid rain and snow by using the developed model.

INTRODUCTION

The problem of acid rain has become a complex social, political and environmental problem. Therefore, much scientific research has been devoted to solve the problem of acid rain. In the Hydrosience and Hydraulic engineering field of Japan, we have published several papers regarding acid rain. Shiba et al. (10) treated the detail process in which acid substances are scavenged by cloud drops. Atsuta et al. (1) obtained the data of water quality of rainfall on a small time scale. They compared the differences between the rain out process and the wash out process using data. Ii et al. (5) have studied the spatial variation of dissolved substances and isotopes in raindrops. Currently, there is much data available and much knowledge regarding the acid rain processes. Therefore, a numerical model for predicting acid rain is required. Hereafter, this model will be referred to as the acid rain model.

Rutledge and Hobbs (8) have developed the numerical weather prediction model. The model adopted the bulk water type microphysical process method, which is known as the bulk method. The bulk method calculates the mixing ratio of precipitation particles which are classified by particle type such as raindrop, cloud drop, cloud ice and graupel. Rutledge, Hegg and Hobbs (9) have developed a numerical acid rain model based on the bulk water method of Rutledge and Hobbs (8). In Japan, some acid rain models have been developed and most of them use the bulk method for calculating the cloud microphysics. They also adopted the chemical processes based on the ones used by Rutledge, Hegg and Hobbs (9). Kitada et al. (6) have developed the two-dimensional acid rain model which utilizes the bulk method. The Eulerian gridpoint model, or the so called EURAD (3), has been developed by EUROTRAC (2). It was based on MM5 developed by NCAR and PSU, USA. EURAD (3) has been used to study the movement of chemical processes in meso alpha to beta scale in Europe. Wang et al. (13) also have developed an acid rain model based on MM5 using the bulk method.

On the other hand, we use another method for taking in account of cloud microphysics. By using the bin method, the number concentration of precipitation particles which are classified by diameter as well as particle type is calculated. In other words, the size distribution of precipitation particles is calculated by means of the bin method. We calculate the time series variation of size distribution by using the bin method. Size distribution of precipitation particles is an important factor to consider when calculating the acid rain processes, because the rate of scavenging the chemical substances by the particles is a function of the particle diameter.

In this study, we develop an acid rain model that utilizes the bin method. The model for the dynamic processes is the two-dimensional non-hydrostatic model using terrain-following coordinates. Moreover, the model for the chemical processes based on the ones used by Rutledge, Hegg and Hobbs (9) has been developed in order to utilize the bin method. We also investigated the effects of topography on acid rain by considering the movement of chemical substances and mechanism of chemical reaction in clouds.

OUTLINE OF THE NUMERICAL ACID RAIN MODEL

Numerical Model for Resolving a Cloud

The basic concept of the numerical acid rain model was developed by Takahashi (11), Takahashi et al. (12) and Oishi et al. (7). This model is applied to two dimensional vertical cross section in which the horizontal axis is set parallel with the wind direction.

The model for the dynamic processes is characterized by non-hydrostatic model, anelastic (AE) assumption and terrain following coordinate using tensor analysis. The microphysical processes in the model are carried out by the bin method.

In order to apply the bin method to the model, the precipitation particles are classified into water drop, graupel, hail and snow. Water drop, graupel and hail are assumed to be the sphere in the model. A snow particle is assumed to be a disk. Each spherical precipitation particle is classified into 45 classes according to their diameters. The disk type particle is classified into 21 classes by the diameter and 5 classes by the thickness. The microphysical model consists of the condensation process, aggregation process, freezing process, riming process and melting process. The breakup process of the precipitation particles is not considered in the model. The details of the microphysical model are discussed in Oishi et al. (7)

Table 1: Correspondence between the precipitation particle type of Rutledge, Hegg and Hobbs and the type of Takahashi,

phase	Takahashi		Rutledge et al.
liquid	water drop	small	cloud drop
		large	rain drop
ice	disk	small	cloud ice
		large	snow
	graupel		graupel
	hail		

Chemical Source and Sink

The chemical substance balance model in the numerical model of this study is based on the ones used by Rutledge, Hegg and Hobbs (9). We changed the calculation process regarding the size distribution of precipitation particles. Rutledge, Hegg and Hobbs (9) give a priori the parameterized size distribution to calculate Eq. 3 mentioned later, since they use the bulk method. On the other hand, we integrated Eq. 3 numerically by using

the calculated size distribution and falling velocity of the precipitation particles. The correspondence between the precipitation particle type of Rutledge, Hegg and Hobbs (9) and that of Takahashi (11) is shown in **Table 1**.

Table 2 shows the chemical substances treated in this study. These substances are transported by advection before being scavenged by precipitation particles. They are transported by advection with precipitation particles after being scavenged and they fall with particles.

The chemical substances are dissolved into precipitation particles by the following processes, 1) nucleation, 2) absorption of gas and 3) scavenging of the chemical substance during precipitation. When precipitation particles change their phases (water, ice and water vapor), the dissolved substances also change their phases. The main

Table 2: Initial and boundary condition for numerical simulation,

substances	$Q_s(0)$	$Q_s(0)$	HI_s
s	[g/g]	[ppb]	[km]
SO ₂	4.3×10^{-9}	1.95	2.0
SO ₄ ²⁻	3.1×10^{-9}	–	3.5
NH ₄ ⁺	1.6×10^{-8}	–	3.5
H ₂ O ₂	5.9×10^{-10}	0.506	∞
NO ₃ ⁻	7.7×10^{-10}	–	3.5
HNO ₃	1.7×10^{-9}	0.780	2.0
PAN	4.2×10^{-9}	0.014	∞

details concerning the balance of chemical substances are as follows:

a) Production of the sulfate in precipitation particles,

Sulfate ion is made by oxidation of SO₂ which is dissolved in precipitation particles. The amount of dissolved SO₂ is calculated by **Eq. 1**.

$$\begin{aligned}
 PC_1 &= 10^3 C_{1i} Q_{\text{SO}_2} q_{\text{end},i} \\
 C_{1i} &= \frac{1.75 \times 10^{-14}}{[H_i]} \exp\left(\frac{5.19 \times 10^3}{T}\right)
 \end{aligned} \tag{1}$$

where, PC_1 = the rate of sulfur dioxide which transforms from the gas phase SO₂ to dissolved SO₂ [g(SO₂)/g(air)/s]; $q_{\text{end},i}$ = the rate of condensation of water vapor to precipitation particles [g(water)/g(air)/s]; i = the type of precipitation particles (cloud drops, raindrops etc.); Q_{SO_2} = the mixing ratio of SO₂ [g(SO₂)/g(air)], $[H_i]$ = concentration of H⁺ in the precipitation particle i [mols/ℓ]; and T = the temperature [K]. The rate of sulfate ion which is made by oxidation is calculated by **Eq. 2**.

$$\begin{aligned}
 PC_2 &= 10^3 C_{2i} Q_{\text{SO}_2} Q_i \\
 C_{2i} &= \frac{5.37 \times 10^{-19}}{([H_i])^{0.9}} \exp\left(\frac{6.778 \times 10^3}{T}\right) \\
 &+ (Q_{\text{H}_2\text{O}_2,i}/Q_i) \frac{2.67 \times 10^{-2}}{([H_i])^{0.27}} \exp\left(\frac{2.41 \times 10^3}{T}\right)
 \end{aligned} \tag{2}$$

where, PC_2 = the rate of sulfate ion which is made by oxidation [g(SO₄²⁻)/g(air)/s]; $Q_{\text{H}_2\text{O}_2,i}$ = the mixing ratio of H₂O₂ in precipitation particles of type i ; and Q_i = the mixing ratio of precipitation particle i .

b) Absorption of the nitric acid vapor in the precipitation particles.

Since nitric acid vapor is highly dissolvable in water, all this acid vapor is assumed to be absorbed into water. If there is a cloud drop and a raindrop in the air, nitric acid vapor is absorbed in the cloud drop. In the low temperature atmosphere, where no precipitation particle of liquid type exists, nitric acid vapor is absorbed into precipitation particles of ice type, such as snow, graupel and hail. The rate of nitric acid vapor which is absorbed by the ice type particles is calculated by Eq. 3,

$$PG = Q_{\text{HNO}_3} \sum_{D_d} 2\pi \times 0.75 \times K_D D_d (0.65 + 0.44 Sc^{1/3} Re^{1/2}) N(d) \quad (3)$$

$$Sc^{1/3} Re^{1/2} = \left(\frac{\nu}{D_d}\right)^{1/3} \left(\frac{V_d 2D_d}{\nu}\right)^{1/2}$$

where, PG = the rate of nitric acid vapor which transforms from the gas phase to dissolved NO_3 [$\text{g}(\text{NO}_3)/\text{g}(\text{air})/\text{s}$]; K_D = the diffusion coefficient of nitric acid vapor in the air ($1.1 \times 10^4 [\text{m}^2/\text{s}]$); Q_{HNO_3} = the mixing ratio of nitric acid vapor [$\text{g}(\text{HNO}_3)/\text{g}(\text{air})$]. d = the class of precipitation particles, which is classified according to the diameter and the type of particles (snow, graupel and hail); D_d = the diameter of a precipitation particle of class d [m]; $N(d)$ = the number concentration of precipitation particles of class d [$1/\text{m}^3$]; ν = the kinematic viscosity of air ($1.34 \times 10^{-5} [\text{m}^2/\text{s}]$); and V_d = the terminal velocity of the precipitation particles of class d [m/s]. In Eq. 3, the unit of m, kg and second is used for adopting the equation in Rutledge, Hegg and Hobbs (9). In this study, we mainly use the unit of cm, g and second in the dynamic and microphysical processes.

APPLICATION AND DISCUSSION

At this stage of our investigation, we compare the calculated concentration of chemical substances with observed data in order to confirm the validity of numerical model. Moreover, we discuss the effects of mountainous topography on the movement of chemical substances in the cloud.

Initial and Boundary Conditions of Chemical Substances

The initial and boundary conditions of chemical substances are given by exponential function

$$Q_s = Q_s(0) \exp(-h/\text{HI}_s) \quad (4)$$

where, s = the kind of chemical substances; $Q_s(0)$ = the mixing ratio of the substance s at the ground surface [$\text{g}(\text{substance})/\text{g}(\text{air})$], and HI_s = the coefficient of decrease for the substance s [km]. Eq. 4 is based on Rutledge, Hegg and Hobbs (9). Table 2 shows the values of $Q_s(0)$ and HI_s for each chemical substance s .

Comparison between Calculated Result and Observed Data

We compared the calculated concentration of chemical substances with observed data in order to validate the numerical model. Table 3 shows the observed and calculated sulfate ion concentration. Table 4 shows the nitrate ion concentration. In these tables, the quantity has a unit of $[\mu\text{eq}/\ell]$. In the fifth column of Table 3 and Table 4, "snow" denotes the situation of snow (low temperature) and "c.c." denotes the convective cold rain.

The observed data used for this comparison is the data of the third investigation for countermeasures against acid rain. The investigation was made by Ministry of Environment from 1991 to 1997. The places of observation were selected in this paper as follows, 1) Niigata which is located along the sea of Japan where acid rain and acid snow fall in large amounts in winter, 2) Osaka which is a typical urban area, 3) Yahata in Kyoto prefecture, which is a rural areas near Osaka. The averaged amount is the monthly average weighted by the rainfall amount.

The calculated results were 11 cases, that is, eight cases of convective rainfall, two cases of stratiform rainfall and one case of snow. The calculated concentration of sulfate ion and nitrate ion were averaged by weighting the

Table 3: Observed and calculated concentration of sulfate ion [$\mu\text{eq}/\ell$],

	Observed			Calculated
	Niigata	Osaka	Yawata	Model
average	57.6	30.0	32.3	18.3
max. (month)	139 (Apr)	47.7 (Dec)	56.0 (Dec)	30.0 (snow)
min. (month)	14.9 (Jul)	17.4 (Sep)	19.7 (May)	10.2 (c.c.)

Table 4: Observed and calculated concentration of nitrate ion [$\mu\text{eq}/\ell$],

	Observed			Calculated
	Niigata	Osaka	Yawata	Model
average	15.3	12.3	19.1	13.7
max. (month)	39.9 (Apr)	20.7 (Dec)	27.9 (Nov)	22.5 (snow)
min. (month)	4.91 (Sep)	6.13 (Oct)	10.2 (Jan)	7.7 (c.c.)

precipitation amount. The eight cases of convective rainfall consisted of calculations with a mountain (or without a mountain), strong horizontal wind (or weak horizontal wind), and cold rain (or warm rain). The two cases of stratiform rainfall consisted of either calculation with a mountain or without a mountain.

The findings of the observed data show that a high concentration of acidic ion occurs in the season with the smallest amount of rainfall. The same result was found in the calculated data. This fact suggests that the amount of chemical substance does not depend proportionally on the amount of rainfall.

As for the order of magnitude, the calculated sulfate ion concentrations are the same as the observed ones. It should be noted that the concentration of chemical substances in the atmosphere during the observation period was not known. Nevertheless, the seasonal variation of the concentration of sulfate ion was checked. Both calculated results and observed data had the same characteristics from a seasonal point of view. Since there was not much difference in the calculated concentration of chemical substances in the atmosphere between winter and summer, one can conclude that the model simulated the chemical balance very well.

There is no conspicuous difference in nitrate ion concentration between the calculated result and the observed data. However, sulfate ion concentration by the model calculation are less than that from observed data. According to Hashimoto (4), the calculated nitrate ion concentration is relatively higher than the observed data, and the calculated sulfate ion concentration is found to be relatively lower than the observed concentration. Hashimoto (4) also reports that the reason for the difference between calculated concentration and observed concentration is not clearly understood. According to Shiba et al. (10), the rate of oxidation, which was calculated using a numerical model while considering the liquid phase oxidation of SO_2 , was 1.6 times larger than the rate calculated without the liquid phase oxidation. He also said that the liquid phase oxidation continues for 100 second. The liquid phase oxidation is one of the most important causes of under-estimating the sulfate ion concentration in the numerical result.

The following discussion focuses on the movement of sulfate ion, since sulfate ion is the main source of acid rain. It should be noted that the temporal and spatial distribution of sulfate ion and nitrate ion is qualitatively the same in the calculated result. Therefore, the following discussion is also relevant to the movement of nitrate ion.

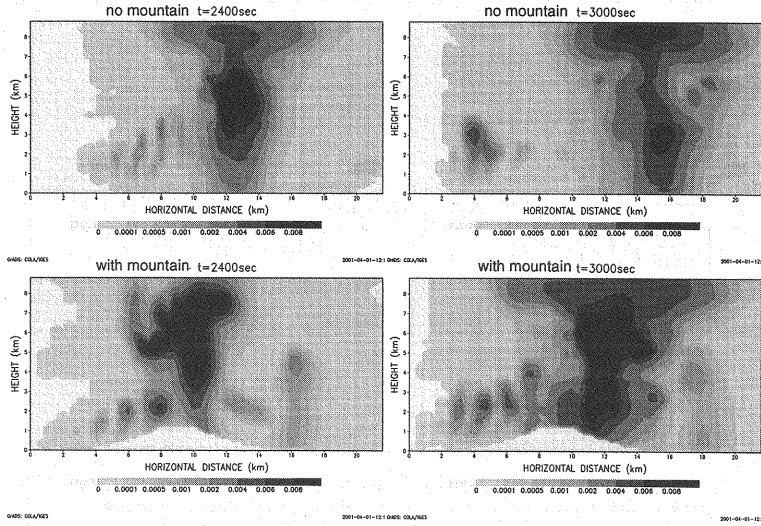


Fig. 1: Cross-sectional distribution of water mixing ratio [g/g].

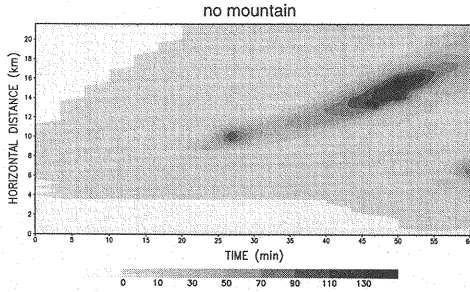


Fig. 2: Time series variation (x-axis) and spatial distribution (y-axis) of rainfall intensity calculated without a mountain [mm/hr].

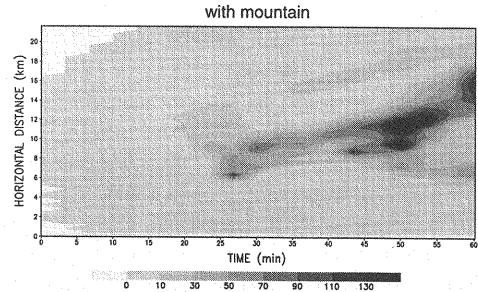


Fig. 3: Time series variation (x-axis) and spatial distribution (y-axis) of rainfall intensity calculated with a mountain [mm/hr].

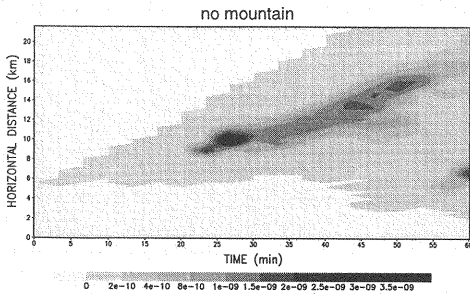


Fig. 4: Time series variation (x-axis) and spatial distribution (y-axis) of sulfate ion fall intensity (no mountain) [g/cm²/s].

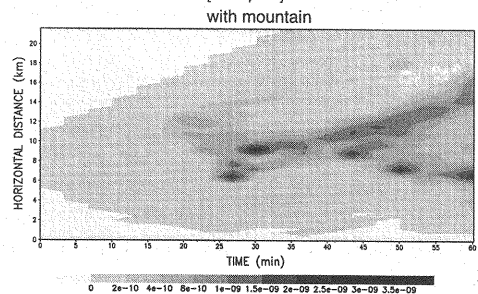


Fig. 5: Time series variation (x-axis) and spatial distribution (y-axis) of sulfate ion fall intensity (with a mountain) [g/cm²/s].

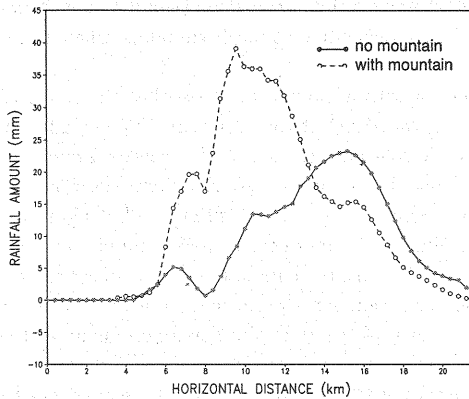


Fig. 6: Spatial distribution of time-integrated amount of rainfall [mm].

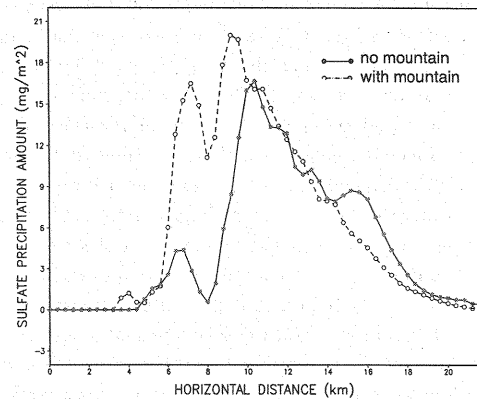


Fig. 7: Spatial distribution of time-integrated amount of sulfate ion deposition [mg/m²].

The Effect of Topography on the Deposition of Sulfate Ion by Convective Rainfall

At the next stage of our study, the effects of topography on the deposition of sulfate ion under the atmospheric condition of convective rainfall are investigated. A comparison is made with respect to topography between mountain and flat bottom. In the case of mountain topography, a two-dimensional bell shaped mountain (elevation is 1600m) is given as a bottom condition. In the case of a flat bottom, a saturated high temperature atmosphere region, which is called a bubble, is given at the lower layer of the calculation field in order to make an initial cumulus. The Brunt-Väisälä frequency of the initial and boundary condition of the atmosphere is 10^{-4} [1/s]. The surface temperature is 300[K]. Water vapor profile is 87% of RH at the surface, 99% at 1200m. Moreover, the higher the altitude, the greater the decrease in humidity above 1200m level.

The effects of topography are investigated by the total amount of precipitation and the total amount of sulfate ion deposition. **Fig. 1** shows the cross-sectional distribution of the mixing ratio of cloud particles which are calculated without a mountain (upper section) and with a mountain (lower section). **Fig. 2** shows the time series variation of rainfall intensity calculated without a mountain. **Figs. 3** shows the time series variation with a mountain. **Figs. 4 and 5** show the time series variation of spatial distribution of sulfate ion fall intensity. **Figs. 6 and 7** show the spatial distribution of time-integrated amount of rainfall and sulfate deposition, respectively. In **Figs. 6 and 7**, the solid line refer to the results without a mountain and the broken line refers to the one with a mountain.

First, we discuss the time-integrated amount of precipitation. **Fig. 6** shows that the spatial distribution without a mountain is a mild curve and has a peak at about the 15km point. **Fig. 6** shows that the distribution with a mountain is a sharp curve and has a peak at about the 10km point. **Fig. 1** shows that the cloud top elevation is higher than 5km regardless of mountain topography. This finding indicates that the cloud consists of ice phase particles such as graupel and hail as well as liquid phase particles. Therefore, precipitation is cold rain (Bergeron-Findeisen rain).

Second, the time-integrated amount of sulfate ion deposition is discussed. **Fig. 7** shows that the sulfate ion deposition without a mountain becomes the maximum at the 10km point, where the strong rainfall begins. **Fig. 7** shows the sulfate ion deposition with a mountain becomes the maximum at the 10km point and the large amount of sulfate ion deposition is shown at the 6-8km point. The effects of topography on the sulfate ion deposition are explained as follows.

The upper section of **Fig. 1**, which refers to the calculation without a mountain, shows how the convective cloud develops into the mature stage and how rain falls as a shower. After the shower, the cloud is moved by wind and rain becomes weaker. For sulfate ion deposition, large amounts of sulfate ion are stored in the mature convective cloud and then falls. Therefore, first rainfall at the 10km point contains much sulfate ion as shown in **Fig. 4**. This is the mechanism of the sulfate ion deposition without a mountain (solid line of **Fig. 7**) which

becomes the maximum at the 10km point. For leeward of the 10km point, rainfall contains the sulfate ion of equal concentration in **Fig. 4**. Therefore, there is a small peak of sulfate ion deposition at the 16km point, where rainfall becomes the maximum as shown by the solid line in **Fig. 7**.

The lower section of **Fig. 1**, which refers to the calculation with a mountain, shows that the convective cloud is matured enough and it rains at the leeward slope (the 10km point) of the mountain. The cloud unites with the following convective cloud. It rains at the same point. It continues to rain at the leeward slope of the mountain, which causes the sulfate ion deposition to increase. This is the mechanism of sulfate ion deposition with a mountain (the broken line of **Fig. 7**) for explaining the maximum sulfate ion deposition at the 10km point. The developing cloud at the windward of the mountain (the 6-8km point) produces a weak rainfall. The weak rainfall contains relatively large amounts of sulfate ion, because wind brings the sulfate ion and no cloud exists at the windward. Therefore, time integrated amounts of sulfate ion deposition exhibits the second peak at the 6-8km point. The ratio of quantity of sulfate ion deposition at the second peak point to the maximum amount of the deposition with a mountain is larger than that without a mountain.

These results lead to the conclusion that the effects of mountainous topography on the sulfate ion deposition are stronger than the effects on the total amount of precipitation.

CONCLUSIONS

In this study, we developed a numerical model for predicting acid rain and snow using the bin method and then we obtained the following results by applying this method to some acid precipitations.

First, we developed the numerical model for resolving a cloud. This model describes the scavenging process of chemical substance such as sulfur dioxide and nitric acid. We also developed a transport model that represents the transport process of chemical substances for application of the bin method. Second, by making a comparison between calculated result and observed data, the numerical results indicate that the model can predict reasonably well the nitrate ion concentration. On the other hand, the model calculations produce less sulfate ion concentration than the observed value. The tendency is the same as the results of the other numerical model for acid rain. Finally, by application of the numerical model, we found that the effects of topography on sulfate ion deposition by the convective rainfall are strong. Findings of this study indicate the effects of topography on time-integrated amount of sulfate ion deposition is stronger than the effects on the amount of rainfall.

We hope that the findings of this study and the numerical model can contribute to our understanding of the mechanism of acid rain and snow processes.

Acknowledgement

The present study was financially supported by Grants-in-Aids (10450182 Representative: Shuichi IKEBUCHI) of the Japan Society for the Promotion of Science (JSPS).

REFERENCE

1. Atsuta, Y., Y. Sakamoto and K. Nishida : A study on water qualities of acid rain based on multi variate analysis and temporal change analysis for ion concentration ratio, Annual Journal of Hydraulic Engineering, JSCE, Vol.45, pp.283-288, 2001. (in Japanese)
2. Borrell, P. and P. Grennfelt : EUROTRAC - Organization Structure and Achievements, Transport and Chemical Transformation of Pollutants in the Troposphere, Springer, pp.3-18, 2000.
3. Ebel, A., H. Elbern, H. J. Jakobs, M. Memmesheimer, M. Laube, A. Oberreuter and G. Piekorz : Simulation of Chemical Transformation and Transport of Air Pollutants with the Model System EURAD, Tropospheric Modelling and Emission Estimation, pp.27-45, 1997.
4. Hashimoto, Y. : Global environmental problem around us, Corona-sha, pp.40-43, 1997. (in Japanese)
5. Ii, H., T. Hirata, N. Sahara and K. Fushii : Chemical composition, hydrogen and oxygen isotopic ratios of precipitation in Wakayama and Osaka prefectures, Annual Journal of Hydraulic Engineering, JSCE, Vol.45, pp.289-294, 2001. (in Japanese)
6. Kitada, T., P. C. S. Lee and H. Ueda : Numerical modeling of long range transport of acidic species in association with meso- β -convective clouds across the Japan sea resulting in acid snow over coastal Japan-I, Model description and qualitative verifications. Atmospheric Environment, Vol.27A, pp.1061-1076, 1993.
7. Oishi, S., Y. Kitani, E. Nakakita and S. Ikebuchi : Numerical approach on effect of topography to severe rainfall using non-parameterized cloud microphysics model, Annual Journal of Hydraulic Engineering, JSCE, Vol.41, pp.117-122, 1997. (in Japanese)

8. Rutledge, S.A and P.V.Hobbs : The mesoscale and microscale structure and organization of clouds and precipitation in midlatitude cyclones. XII: A diagnostic modeling study of precipitation development in narrow cold-frontal rain bands. *Journal of Atmospheric Science*, Vol.41, pp.2949-2972, 1974.
9. Rutledge, S.A, D.A.Hegg and P.V.Hobbs : A Numerical Model for Sulfur and Nitrogen Scavenging in narrow Cold-Frontal Rainbands, 1. Model Description and Discussion of Microphysical Fields, *Journal of Geophysical Research*, Vol.91-D13, pp14385-14402, 1986.
10. Shiba, S., Y.Hirata and S.Yagi : Effect of oxidation on acidification of cloud droplet in condensational growth, *Annual Journal of Hydraulic Engineering, JSCE*, Vol.45, pp.277-282, 2001. (in Japanese)
11. Takahashi, T. : Warm rain, giant nuclei and chemical balance, *Journal of Atmospheric Science*, Vol.33, pp.269-286, 1974.
12. Takahashi, T. and Y.Awata : Cloud development in a two-dimensional cloud model with detailed microphysics, *Annals Disaster Prevention Research Institute, Kyoto University*, Vol.36-B2, pp.189-217, 1993 (in Japanese)
13. Wang, Z., T.Maeda and M.Hayashi : A nested air quality prediction modeling system for urban and regional scales: Application for high-ozone episode in Taiwan, *Abstract book of Acid rain 2000*, p.28, 2000.

APPENDIX - NOTATION

The following symbols are used in this paper:

d	=	the class of precipitation particles, which is classified by the diameter; and the type of particles (water drop, snow, graupel and hail)
D_d	=	the diameter of precipitation particles of class d [cm];
$[H_i]$	=	the concentration of H^+ in precipitation particle i [mols/ ℓ];
HI_s	=	the coefficient of decrease of initial profile of the substance s [km];
i	=	the type of precipitation particles (cloud drops, raindrops, etc.);
K_D	=	the diffusion coefficient of nitric acid vapor in air (1.1×10^5 [m ² /s]);
$N(d)$	=	the number concentration of precipitation particles of class d [1/cm ³];
PC_1	=	the rate of sulfur dioxide transformation from gas phase SO_2 to dissolved SO_2 [g(SO_2)/g(air)/s];
PC_2	=	the rate of sulfate ion made by oxidation SO_4^{2-} [g(SO_4^{2-})/g(air)/s];
PG	=	the rate of nitric acid vapor which is absorbed by the ice type particles [g(NO_3)/g(air)/s];
$q_{cnd,i}$	=	the rate of condensation of water vapor to the precipitation particles [g(water)/g(air)/s];
$Q_{H_2O_2,i}$	=	the mixing ratio of H_2O_2 in precipitation particle of type i [g(H_2O_2)/g(air)];
Q_{HNO_3}	=	the mixing ratio of nitric acid vapor [g(HNO_3)/g(air)];
Q_i	=	the mixing ratio of precipitation particle of type i [g(particle)/g(air)];
$Q_s(0)$	=	the mixing ratio of substance s at the ground surface [g(substance)/g(air)];
Q_{SO_2}	=	the mixing ratio of SO_2 [g(SO_2)/g(air)];
s	=	the kind of chemical substance (SO_2 etc.);
T	=	the temperature [K];
V_d	=	the terminal velocity of the precipitation particles of class d [cm/s]; and
ν	=	the kinematic viscosity of air (1.34×10^{-5} [m ² /s]).

(Received June 10, 2002 ; revised September 10, 2002)